8908 *Biochemistry* **2009,** *48,* 8908–8919
DOI: 10.1021/bi9006397

BIOCHEMISTRY
including biophysical chemistry & molecular biology
Article

Two Disaccharides and Trimethylamine *N*-Oxide Affect Aβ Aggregation Differently, but All Attenuate Oligomer-Induced Membrane Permeability[†]

Wei Qi,[‡] Aming Zhang,[‡] Theresa A. Good,[§] and Erik J. Fernandez*,[‡]

[‡]*Department of Chemical Engineering, University of Virginia, Charlottesville, Virginia 22904, and* [§]*Department of Chemical and Biochemical Engineering, University of Maryland Baltimore County, Baltimore, Maryland 21250*

Received April 14, 2009; Revised Manuscript Received July 24, 2009

ABSTRACT: Interaction between aggregates of amyloid beta protein (Aβ) and membranes has been hypothesized by many to be a key event in the mechanism of neurotoxicity associated with Alzheimer's disease (AD). Proposed membrane-related mechanisms of neurotoxicity include ion channel formation, membrane disruption, changes in membrane capacitance, and lipid membrane oxidation. Recently, osmolytes such as trehalose have been found to delay Aβ aggregation *in vitro* and reduce neurotoxicity. However, no direct measurements have separated the effects of osmolytes on Aβ aggregation versus membrane interactions. In this article, we tested the influence of trehalose, sucrose and trimethylamine-*N*-oxide (TMAO) on Aβ aggregation and fluorescent dye leakage induced by Aβ aggregates from liposomes. In the absence of lipid vesicles, trehalose and sucrose, but not TMAO, were found to delay Aβ aggregation. In contrast, all of the osmolytes significantly attenuated dye leakage. Dissolution of preformed Aβ aggregates was excluded as a possible mechanism of dye leakage attenuation by measurements of Congo red binding as well as hydrogen−deuterium exchange detected by mass spectrometry (HX-MS). However, the accelerated conversion of high order oligomers to fibril caused by vesicles did not take place if any of the three osmolytes presented. Instead, in the case of disaccharide, osmolytes were found to form adducts with Aβ, and change the dissociation dynamics of soluble oligomeric species. Both effects may have contributed to the observed osmolyte attenuation of dye leakage. These results suggest that disaccharides and TMAO may have very different effects on Aβ aggregation because of the different tendencies of the osmolytes to interact with the peptide backbone. However, the effects on Aβ membrane interaction may be due to much more general phenomena associated with osmolyte enhancement of Aβ oligomer stability and/or direct interaction of osmolyte with the membrane surface.

Mounting evidence suggests that interaction between aggregated amyloid beta protein (Aβ) and the neuronal membrane is central to Alzheimer's disease (AD[1]). Aggregated Aβ has been shown to exhibit ion channel activity (reviewed by ref *1*), increase membrane permeability and conductance (*2*−*4*), and enhance lipid oxidation (reviewed by ref *5*). Membranes also have the ability to accelerate the aggregation process (*6*−*8*). Lipid type (anionic, zwitterionic, or cationic), pH and salt concentration, lipid bilayer surface pressure, as well as Aβ aggregated states have all been shown to affect the Aβ−lipid interaction (*3*, *7*−*11*). Particularly, the effect of membranes on the oligomer distribution is critical since neurotoxicity has been found to be a strong function of Aβ aggregation state, with oligomers being more toxic than monomer or fibrillar species (*12*−*16*).

Recently, certain osmolytes, especially trehalose, were found to be effective in slowing the aggregation of several aggregation prone proteins including Aβ (1−40) (*17*), insulin (*18*), W7FW14F (*19*) and polyglutamine containing protein (*20*). More importantly, trehalose was able to increase human neuroblastoma cell (SH-SY5Y) viability in the presence of Aβ aggregates (*17*) and alleviate the polyglutamine induced symptoms in a mouse model of Huntington disease(*20*). Another osmolyte, trimethylamine-*N*-oxide (TMAO), protected MC65 cells under conditional expression of amyloid protein precursor carboxy-terminal fragments (*21*).

Though encouraging results were reported, the effects of osmolytes on Aβ aggregation and oligomer−membrane interactions are not well understood. In the above studies, Congo red, Thioflavin T, and circular dichroism were used to assess the formation of amyloid or β-sheet structure, but these methods could not reveal the distribution of oligomers within a mixture of aggregates. Knowledge of the effects of osmolytes and membranes on the oligomer distribution is important since slowed aggregation could cause accumulation of soluble oligomers, which might be the most neurotoxic oligomeric state (*12*−*17*, *19*, *22*). Detailed measurements of oligomer distributions would help to clarify whether particular osmolytes affect aggregation, oligomer-membrane interactions, or both.

[†]This research was funded by NIH 1R01 NS 042686 to T.A.G. and E.J.F., and in part by award No. 08-3 from the Commonwealth of Virginia's Alzheimer's and Related Diseases Research Award Fund, administered by Virginia Center on Aging, Virginia Commonwealth University.

*Corresponding author. Department of Chemical Engineering, University of Virginia, 102 Engineer's Way, Charlottesville, VA 22904. Phone: (434) 924-1351. Fax: (434) 982-2658. E-mail: erik@virginia.edu.

[1]Abbreviations: AD, Alzheimer's disease; Aβ, Amyloid beta protein; CF, 5(6)-carboxyfluorescein; DCA, dichloroacetic acid; DMSO, dimethylsulfoxide; F, fibril; HMW,high molecular weight oligomer; HX-MS, hydrogen−deuterium exchange detected by mass spectrometry; LUV, large unilamellar vesicles; LMW, low molecular weight oligomer; M, monomer; POPC, palmitoyl-2-oleoyl-sn-glycero-3-phosphocholine; POPG, 1-palmitoyl-2-oleoyl-sn-glycero-3-phospho-rac-1-glycerol [sodium salt]; TFA, trifluoroacetic acid; TMAO, trimethylamine-N-oxide.

 Published on Web 07/28/2009

To explain the beneficial effects of osmolytes on neurotoxicity, mechanisms such as dissociating preformed Aβ aggregates (*17*) or increased protein stability (*20*, *21*) have been proposed. Unfortunately, these results were obtained from different aggregating peptides, osmolytes, and aggregation conditions, making it hard to draw general conclusions about the property of beneficial osmolytes and dominant mechanisms. Consequently, additional studies are needed of different osmolytes under common aggregation conditions, including effects on membrane interactions. Considering the different preferences of TMAO and carbohydrates to interact with peptide backbones (*23*, *24*), we found it interesting and worthwhile to compare their effects on Aβ-membrane interaction with a single model system.

In this work, we have directly compared the effects of two kinds of osmolytes, TMAO and two disaccharides, on Aβ−liposome interactions. Because of the importance of Aβ conformation and aggregation state on such interactions, we prepared different kinds of aggregate distributions prior to liposome exposure, as opposed to the simultaneous aggregation and liposome interaction studies (*10*, *25*). To define composition of the aggregates in the samples, we have exploited a methodology based on hydrogen exchange detected by mass spectrometry (HX-MS) (*26*). Control studies in the absence of liposomes were also performed to distinguish the effects of osmolytes on Aβ aggregation vs Aβ−liposome interactions.

On the basis of the results, trehalose and sucrose were found to delay Aβ aggregation significantly in the absence of liposomes, whereas TMAO did not. In contrast, all three osmolytes abolished the acceleration of Aβ aggregation caused by liposomes and also reduced dye leakage from liposomes. Thus, while the osmolytes had different effects on aggregation in the absence of liposomes, all three osmolytes increased membrane integrity and delayed membrane-induced fibril formation. Sugar−Aβ complexes detected in mass spectra suggested that direct Aβ−carbohydrate interactions could play a role in their different effects on aggregation.

MATERIALS AND METHODS

Materials. Aβ(1−40) was purchased from Anaspec, Inc. (San Jose, CA) as 1.0 mg lyophilized aliquots. POPC (1-palmitoyl-2-oleoyl-*sn*-glycero-3-phosphocholine) and POPG (1-palmitoyl-2-oleoyl-*sn*-glycero-3-phospho-*rac*-1-glycerol [sodium salt]) were obtained from Avanti (Alabaster, AL) and used without further purification. Trehalose and sucrose were from Fisher (Fair Lawn, NJ). 5(6)-Carboxyfluorescein and trimethylamine-*N*-oxide were from Acros Organics (Fair Lawn, NJ). One lot of Aβ was used for all studies. Others materials were obtained from Sigma unless otherwise specified.

Sample Preparation. Stock solutions of Aβ were prepared by dissolving an aliquot of Aβ in 100 μL of 0.1% trifluoroacetic acid (TFA, Fluka, Buchs, Switzerland) to a concentration of 10 mg/mL at 25 ± 0.5 °C. After 45 min of dissolution in TFA, fresh samples were made by diluting the stock to a final concentration at 100 μM in PBS (10 mM NaH_2PO_4 and 150 mM NaCl at pH 7.4). Aged samples were prepared by diluting TFA stock in PBS as described above and then quiescently incubated at 37 °C for 4 h, 10 h, 24 h, or 72 h before labeling. For the samples incubated with osmolytes, osmolytes were added at the same time as PBS was added to TFA stocks, to ensure that no aggregation took place prior to osmolyte addition. Osmolyte concentrations were 250 mM unless otherwise specified. This concentration was used to keep the Aβ/osmolyte molar ratio consistent with the one previously reported to delay Aβ aggregation as detected by Thioflavin T (ThT) fluorescence assay (*17*).

Congo Red Binding Assay. Congo red stock solution (120 μM in PBS) first was passed through a 0.22 μm filter and then mixed with a 100 μM Aβ sample at a volume ratio 1:9. After 45 min of incubation at 25 °C, absorbance at 405 and 541 nm was measured with a SpectraMax Plus^{384} Microplate Reader (Molecular Devices, Sunnyvale, CA). For each time point, at least three replicates were measured. The molar concentration of Congo red bound to Aβ was calculated by the well-established equation of Klunk et al. (*27*):

$$[\text{CR-A}\beta] = ({}^{541}A_t/47800) - ({}^{403}A_t/68300) - ({}^{403}A_{CR}/86200)$$

Here, ${}^{541}A_t$ and ${}^{403}A_t$ are the total absorbance of the Congo red−Aβ mixtures at 541 and 403 nm, respectively, and ${}^{403}A_{CR}$ is the absorbance of Congo red alone in phosphate buffer with and without osmolytes. In the microplate reader, absorbances at 405 and 540 nm were assumed to be the same as those at 403 and 541 nm (*15*).

Hydrogen Exchange Mass Spectrometry (*HX-MS*). HX-MS analysis of Aβ oligomer distributions was carried out as previously reported (*26*). Briefly, a 5 μL sample was diluted into 45 μL of D_2O (Cambridge Isotope Laboratories, D 99.9%) in a 1.5 mL Eppendorf centrifuge tube. The molar D% in the solvent was 90%, and the pH (as read) was 7.0. Labeling was carried out at ambient temperature for the desired labeling time. Subsequently, a mixture of 150 μL of dimethylsulfoxide (DMSO) and dichloroacetic acid (DCA, Fluka, 95/5 vol/vol) were used to rapidly dissolve aggregates back to the monomer state and quench the labeling reaction at pH 3.5 (*26*, *28*). Finally, the sample was sent through a C8 desalting column (Micro Trap 1 mm ID x 8 mm, Michrom Bioresources, Inc., Auburn, CA). A gradient from 30% to 80% acetonitrile was used to elute the peptide from the C8 desalting column directly into the mass spectrometer at 50 μL/min. Data were collected in positive ion, zoom scan, and profile mode on a Thermo Finnigan LTQ linear quadrupole ion trap mass spectrometer (San Jose, CA) with a standard ESI source. ESI voltage was 4.5 kV, capillary temperature 275 °C, sheath gas flow rate 20 units, and tube lens voltage 135 V. All mass spectra presented were averages of approximately 400 scans. The most abundant +4 state was used for HX analysis, and other charge states (+3, +5, and +6) were also observed.

Liposome Preparation. Either POPC or POPG was prepared in PBS buffer to give multilamellar lipid dispersions. To prepare large unilamellar vesicles (LUVs), the dispersion was subjected to five freeze−thaw cycles in liquid nitrogen and in a 37 °C water bath, followed by extrusion (at least 15 times) through polycarbonate membranes with a 100 nm pore size (Avestin, Ottawa, Canada). To prepare the 5(6)-carboxyfluorescein (CF) loaded liposomes, lipids were dissolved in approximately 90 mM CF in water and put through the same procedure as that described above. After the extrusion step, the free carboxyfluorescein was removed by overnight dialysis at 4 °C against PBS buffer with balanced osmosis pressure inside and outside the lipid vesicles in a Slide-A-Lyzer Dialysis cassette from Thermo (Rockford, IL).

Dye-Leakage Assay Measure by Fluorescence. The release of CF dye from POPG LUVs was measured with a Fluorolog-3 spectrofluorometer (Jobin-Yvon, Edison, NJ) at

excitation and emission wavelengths of 480 and 516 nm, respectively, through a 10 mm cuvette. Preaged fresh, 4 and 72 h Aβ samples (100 μM) in PBS were then added to POPG liposome in PBS, trehalose, sucrose, and TMAO solutions. In the final mixture, the molar ratio of lipid to peptide was 20:1, and osmolytes concentrations were approximately 250 mM. The solution was carefully mixed and further incubated for 1 h at 37 °C to allow the leakage to reach maximum. Previously, others have shown 10 min was sufficient for Aβ(1−42) to induce significant leakage from POPC giant unilamellar vesicles (*29*), and for Aβ(1−40), almost 100% leakage was observed for aged samples within approximately 8 min for PG vesicles (*9*). Relative leakage was expressed as a percentage relative to the total amount of dye release obtained by adding 1% Triton X-100 to the CF loaded vesicles (*29*, *30*). CF loaded LUVs were taken as 0% leakage, which showed only slight leakage (less than 3%) within 1 h of measuring time. Each sample was measured in triplicate.

RESULTS

Osmolytes' Effects on Aβ Aggregation in the Absence of Liposomes. Congo Red Assay. Congo red binding was used to assess the effects of osmolytes on Aβ aggregation under our conditions. Because Congo red binds to extended β-sheet structure and not specifically to any particular aggregates or fibril (*31*), the results were used qualitatively. For PBS controls (Figure 1, filled bar), Congo red intensity quickly reached a maximum after only 4 h of incubation. Even in the freshly prepared Aβ sample, Congo red showed some binding, suggesting the existence of some aggregated intermediate with extended β-sheet structure, possibly an oligomer or protofibril. This rapid assembly is consistent with our previous results from the same lot of Aβ under the same conditions (*26*, *32*). For Aβ samples incubated with osmolytes, the Congo red binding time course was not dramatically different. However, the time at which the maximum Congo red binding observed was later for the osmolyte-containing samples (4 h for PBS; 10 h for TMAO; 72 h for sucrose and trehalose). These results suggest that osmolytes may delay the aggregation to a certain extent. However, the relative amounts of oligomers vs fibrils present could not be assessed from this data.

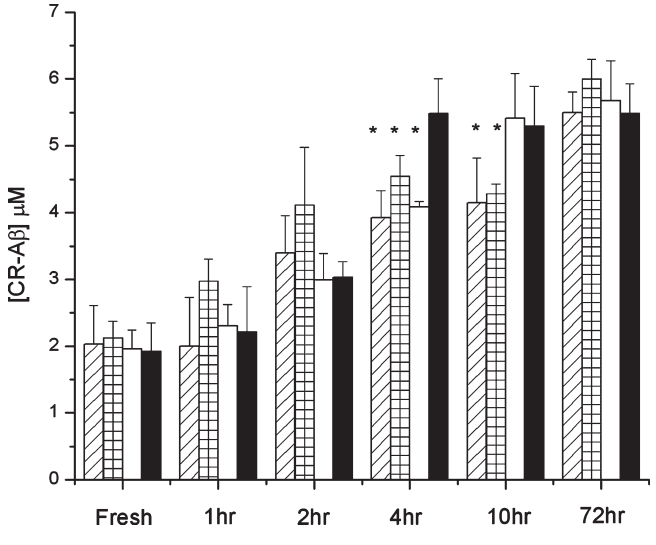

FIGURE 1: Congo red assay for the amount of bound Congo red [CR-Aβ] (see Materials and Methods). Aβ samples were incubated at 37 °C quiescently in PBS (filled bar), trehalose (slashed bar), sucrose (grid bar), and TMAO (open bar). Incubation times are shown as *x*-axis labels. Aβ concentration was 100 μM, and each osmolyte concentration was 250 mM. Asterisks indicate conditions significantly different from those in PBS controls (ANOVA, $p < 0.01$).

HX-MS Measurements of Aggregate Structure Distributions. HX-MS was used to provide complementary information about the distribution of aggregated Aβ structures. We have shown previously that HX-MS can distinguish Aβ in monomeric, low molecular weight (LMW), high molecular weight (HMW), and fibrillar forms (*26*). In the same work, we carefully deconvoluted spectra by typical Gaussian peak fitting and assigned peaks to different aggregated structures based on their degree of deuterium exchange and complementary measurements (*15*, *26*). It should be mentioned that HMW and LMW are both distributions with centroids representing the average mass. Thus, their distributions might be partially overlapped.

Figure 2 compares Aβ structural distributions incubated in the absence and presence of the osmolytes. The Aβ concentration was fixed at 100 μM and osmolyte concentrations were set at 250 mM. At this molar ratio, the inhibition of Aβ aggregation by trehalose has been shown to be efficient (*17*). Aβ samples in PBS without osmolytes that served as controls in this study showed the same trends in distributions as we observed previously (*26*). The top row of Figure 2 shows that the fresh sample contained fully labeled monomer (M) and some partially protected LMW oligomers (L). Samples incubated for longer periods prior to deuterium labeling (Figure 2, 4 h through 72 h) were all mixtures, with a major peak of partially protected HMW oligomers (H) and a growing fibril peak (F) at long times. In the second row of Figure 2, samples of Aβ aggregated with TMAO showed a labeling pattern similar to that of PBS controls at every incubation time point. Markedly different labeling distributions were generally observed for Aβ samples incubated in the presence of trehalose and sucrose. The fresh sample was similar to PBS controls in terms of both initial distribution and dynamics. However, for 4 and 10 h aging times, solvent exposed monomer made up to more than 50% of the distributions for samples incubated with carbohydrate, while the HMW species was the major component in PBS and TMAO-containing samples. After 24 h of incubation with carbohydrate, the monomer still persisted with an abundance of approximately 30%. After 72 h of incubation with carbohydrate, the fibril peak was almost completely absent, and the predominant species was HMW, analogous to the PBS control samples observed at 4 to 10 h aggregation. The rate of aggregation was significantly diminished in the presence of trehalose and sucrose.

For each incubation time, experiments at different subsequent labeling times were used to assess the dissociation rates of the aggregated species formed during the incubation time. Our previous study showed that for PBS controls, LMW oligomers dissociated to the monomer within 10 min, while HMW oligomers and fibrils did not dissociate significantly within a 1 h labeling time (*26*). Aβ incubated with TMAO showed labeling behavior similar to that of PBS controls for samples at all of the incubation time points (data not shown), suggesting the dynamics of Aβ aggregate dissociation were not disturbed by TMAO. However, samples incubated 24 h with trehalose and sucrose showed very different subsequent dynamic labeling behavior. The spectra of fresh Aβ prepared with trehalose were similar to that of fresh PBS controls (Figure 2, left column). With increasing incubation time prior to labeling (4, 10, and 24 h), more LMW were formed, and the time constant for converting LMW to the fully labeled peak was increased. It should be noted that the dissociation rate was measured in labeling buffer

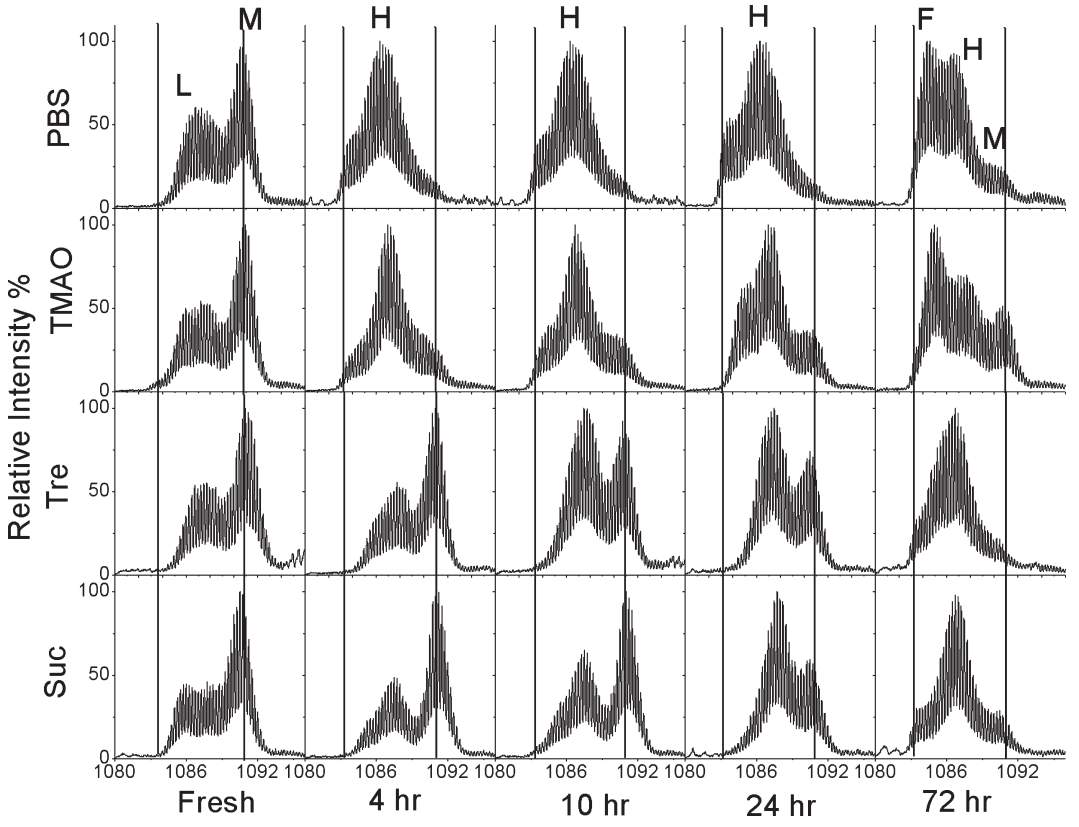

FIGURE 2: Representative hydrogen exchange mass spectra (+4 charge state) for Aβ samples in the absence and presence of TMAO, trehalose (Tre), and sucrose (Suc) at different times of Aβ aggregation. Incubation time points were selected as fresh (0 h), 4 h, 10 h, 24, and 72 h. The Aβ concentration was 100 μM, and each osmolyte concentration was 250 mM. Labeling time was 10 s. Vertical lines in the columns indicated the centroid masses of (gray line) completely unlabeled Aβ and (dark line) fully deuterated Aβ controls. M, L, H, and F indicate the peak arising from monomer, LMW, HMW, and fibril, respectively. Each spectrum was normalized to its own maximum intensity.

prepared without trehalose, and hence, it is a characterization of the aggregate product rather than dissociation during the aggregation with trehalose.

Spectra shown in Figure 3 are representative examples of the labeling dynamics observed after Aβ was incubated for more than 24 h with and without trehalose. For PBS controls (Figure 3, left), HMW oligomer was the predominant species in the sample, with ~20% fibril. Only subtle spectra changes occur along increased labeling time with small increases in the fraction of monomer and a slight reduction in fibril at longer labeling times, indicating that little dissociation occurred. In contrast, samples incubated in trehalose buffer yielded subsequent labeling spectra markedly different in three respects (Figure 3, right). First, no fibril peak was present. Second, the monomer peak was prominent in the spectrum of the sample labeled for 10 s. The less labeled peak in the spectrum of the 10 s labeled sample was ~4.0 Da heavier in mass than the HMW peak in the PBS control spectrum, suggesting that the species were more solvent accessible and/or smaller than the HMW oligomer. The centroid mass for the protected species in the trehalose spectrum (4345.9 ± 1.0 Da) was close to the mass previously reported for LMW for freshly dissolved Aβ (4346.0 ± 0.9 Da) (*26*). Finally, with increased labeling time, the intensity of the more protected oligomer peak decreased while that of the monomer peak increased accordingly in the presence of trehalose. This indicated that the protected species was dissociating to a fully solvent exposed, presumably monomeric state. This is in contrast to the lack of dissociation for Aβ samples incubated for 24 h in the absence of trehalose. Notably, fresh samples in PBS showed a similar labeling pattern indicating dissociation, albeit with a shorter time constant (*26*).

Nonspecific Aβ−Sugar Complex Formation. The above HX-MS data clearly showed that Aβ aggregation could be delayed by trehalose or sucrose but not by the addition of TMAO. Similar observations of delayed Aβ aggregation have been previously reported for carbohydrates (*17*, *19*, *22*). However, the mechanism by which disaccharides influence the aggregation remains unknown. Furthermore, direct measurements of the oligomer−oligomer interactions and/or Aβ−carbohydrate interactions are not available.

One possible line of evidence of saccharide−peptide interactions from this work is the formation of adducts arising from noncovalent association during the electrospray process. Figure 4 shows evidence for such noncovalent association between Aβ and the carbohydrate osmolytes, but not with TMAO. Aβ in PBS buffer (Figure 4, upper left) showed isolated +3, +4, +5, and +6 charge state peaks with centroid masses 1444.18, 1083.45, 867.00, and 722.73, respectively. The +4 charge state was the most abundant signal under electronic spray conditions used in this study, and for clarity, the subsequent discussion focuses on this peak. For Aβ in both trehalose and sucrose solutions, the +4 charge state (m/z 1083.45) was still the strongest peak in the spectra, but it was followed by a series of adduct peaks separated by an average mass of 342.0 ± 0.8 Da (85.5 ± 0.2 m/z at the +4 charge state, and the molecular weight of trehalose and sucrose is 342.3). Adduct peak intensity decreased with increased number of sugar molecules associated with the peptide. In contrast, Aβ samples in TMAO yielded spectra almost identical to that of the PBS sample. No adducts were observed with the mass matching TMAO, even though experiments were conducted under the same experimental

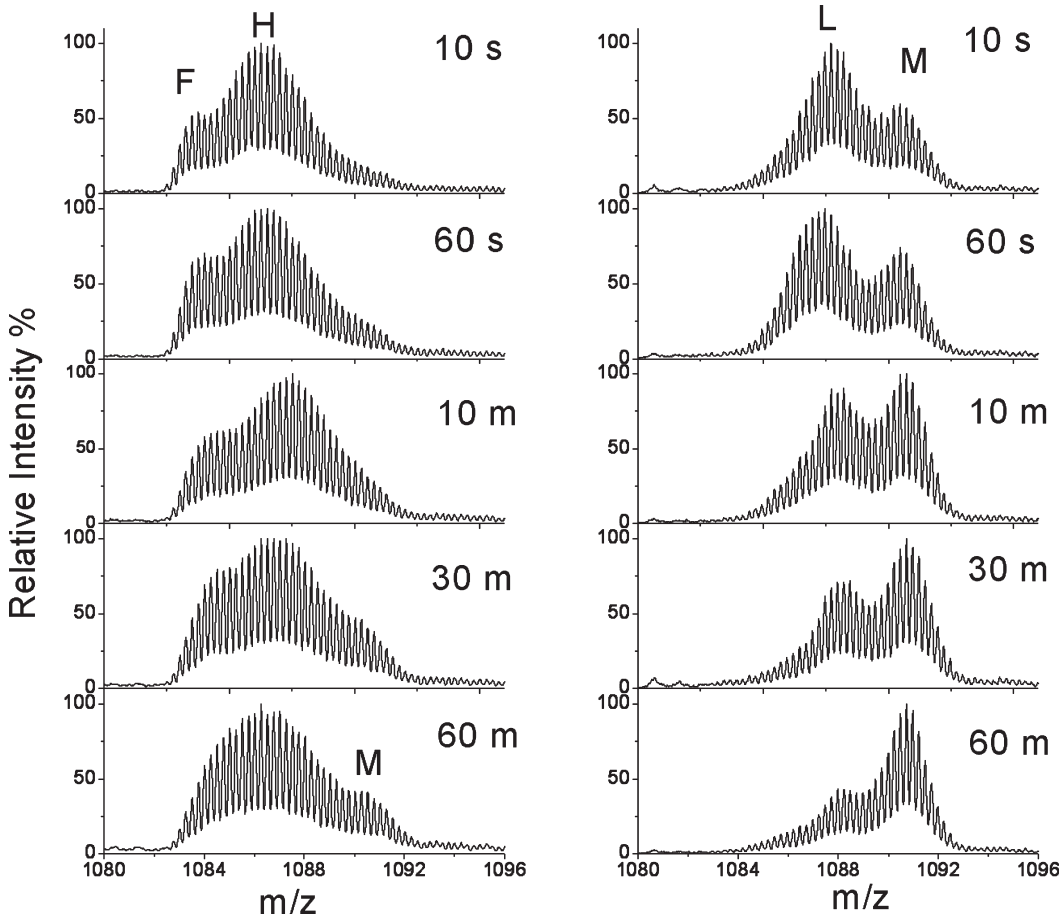

FIGURE 3: Representative hydrogen exchange mass spectra (+4 charge state) for samples incubated for 24 h in PBS (left column) and in trehalose buffer (right column), labeled subsequently for the times indicated. The Aβ concentration during incubation was 100 μM, and the trehalose concentration was 250 mM. Each spectrum was normalized to its own maximum intensity.

procedures and conditions as those for the carbohydrate osmolytes.

Sugar and protein adduct formation during the electrospray ionization (ESI) process have been previously taken to reflect noncovalent interactions between the molecules, probably involving hydrogen bonding (*33*). The abundant −OH groups in sugar molecules and peptide backbones are potential hydrogen bonding candidates. In contrast to the carbohydrates, TMAO is not believed to interact preferentially with the peptide backbone, on the basis of simulation (*34*) and experimental investigations (reviewed in ref *23*). Furthermore, in a recent theoretical transfer free energy model analysis, urea and TMAO represented the two extremes in osmolytes preferentially accumulated or excluded from the protein backbone, respectively. Sugars such as trehalose and sucrose fell in between these two extremes (*23*, *24*). Therefore, the trend in adduct formation observed here was consistent with previous estimates of osmolyte association with the peptide backbone. However, it should be noted that the N−O bond in TMAO has a large dipole; this might allow TMAO to decompose during MS analysis into a positive ion that would be much less likely to form an adduct with the positively charged protein during the electrospray process. This may also contribute to the reduced adduct formation for TMAO.

To test whether the carbohydrate−Aβ interaction is noncovalent, MS experiments were repeated with Aβ concentration fixed at 100 μM, and trehalose concentration adjusted from 100 μM up to 250 mM. As shown in Figure 5, both the intensity and number of adducts increased at the higher trehalose concentrations. This concentration-dependent behavior is typical of the noncovalent complex formation between carbonic anhydrase and a number of sugar molecules (*33*). In addition, the hydrogen exchange behavior was observed to be the same for the main peak and all adducts (see Supporting Information), indicating that the association with trehalose and sucrose was not sufficiently strong and/or long-lived to exclude solvent access to the backbone. Indeed, simulation studies suggest that such a lifetime of the disaccharide−peptide interaction might only be on the scale of approximately nanoseconds (*35*). This would be an insufficient period to exclude D_2O molecules capable of labeling polypeptides in our 10-s labeling period (*26*).

Osmolyte Effects on the Aβ−Liposome Interaction. Carboxyfluorescein Leakage from Liposomes. CF loaded POPG liposomes were used here as an *in vitro* model to detect the effect of preaged Aβ samples on membrane permeability as well as osmolyte influences on Aβ-induced membrane permeability (*9*, *29*). Figure 6 (black bars) shows the impact of preaged Aβ aggregates on induced membrane permeability in the absence of osmolytes. Fresh and 4 h samples led to the marked CF leakage of approximately 70% and 80%, respectively. In contrast, the 72 h sample only resulted in approximately 30% leakage. The combined fraction of HMW and LMW oligomers in each sample prior to mixing with the liposomes was previously reported as 50%, 60%, and 35% for fresh, 4, and 72 h samples, respectively (*26*). Therefore, the Aβ-induced leakage appeared to be roughly correlated with the abundance of HMW and LMW oligomers in each sample.

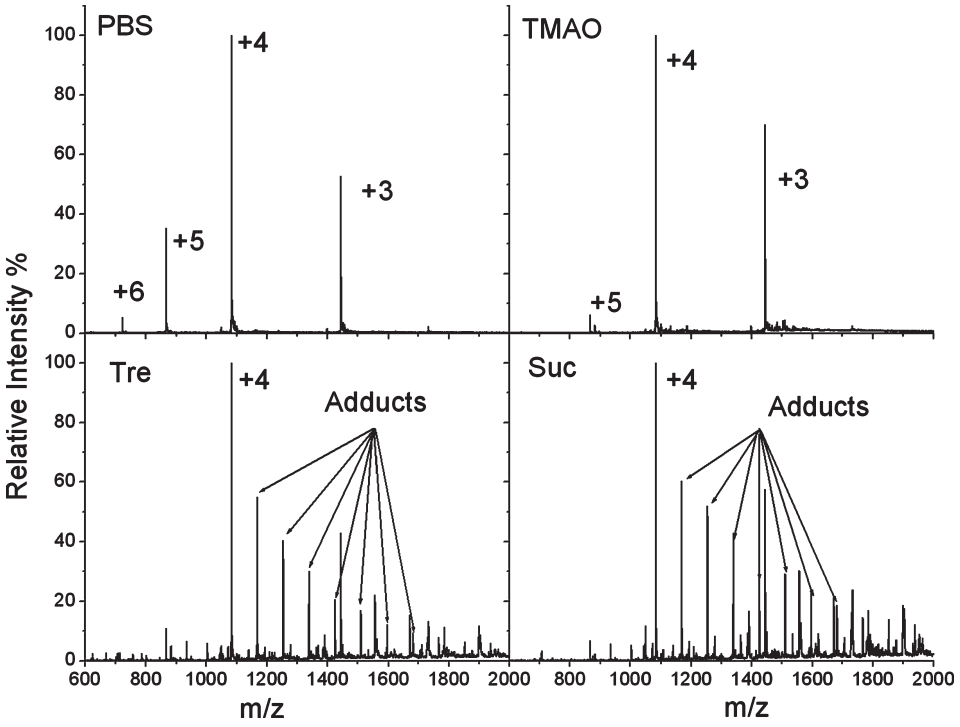

FIGURE 4: Representative mass spectra in full range scan for Aβ samples in PBS, TMAO, trehalose (Tre), and sucrose (Suc) solution. Aβ concentration was 100 μM, and each osmolyte concentration was 250 mM. Samples were treated using the same procedure as that for labeling experiments excluding the D_2O dilution step. Each spectrum is normalized to its own maximum intensity. For Aβ in PBS buffer only, +3, +4, +5, and +6 charge states correspond to observed m/z values of 1444.18, 1083.45, 867.00, and 722.73, respectively. In trehalose and sucrose spectra, the arrows point to the adduct peaks formed with the +4 charge state which are separated by an average mass 342.0 ± 0.8 Da (the approximate molecular weight of both sucrose and trehalose). Adducts were also observed for +3 and +5 charge states.

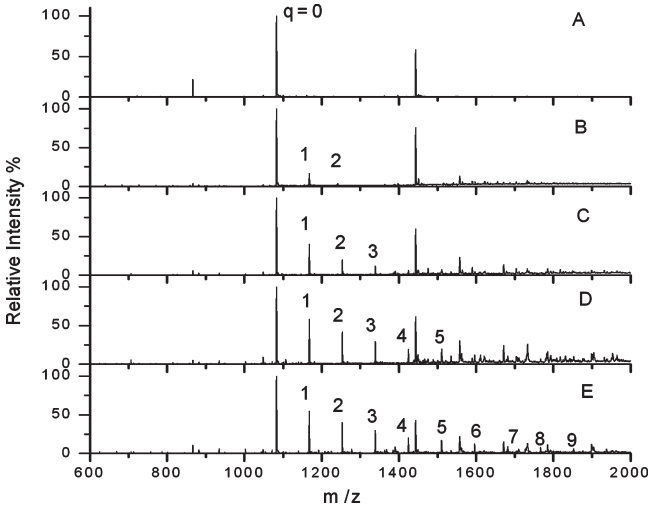

FIGURE 5: Representative mass spectra in full range scan for Aβ samples in different concentrations of trehalose. Aβ concentration was 100 μM and trehalose concentration was 0.1 mM (A), 10 mM (B), 50 mM (C), 100 mM (D), and 250 mM (E). Samples were treated using the same procedure as that used in labeling experiments excluding the D_2O dilution step. q = 0 to 9 was used to indicate the number of the trehalose adducted to Aβ at the +4 charge state. Each spectrum is normalized to its own maximum intensity.

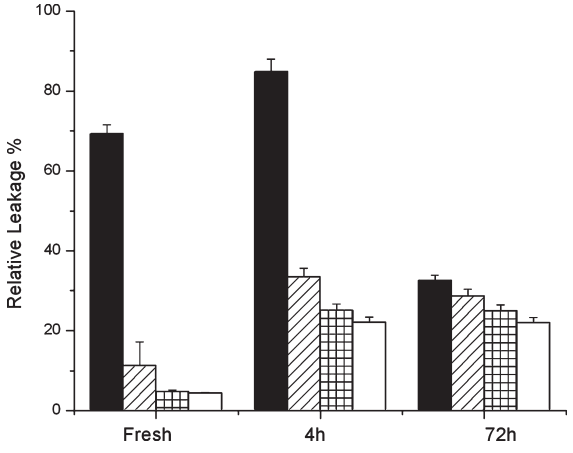

FIGURE 6: Relative percent leakage of CF from POPG LUVs upon incubation with preaged Aβ samples in PBS (filled bar), trehalose (slashed bar), sucrose (grid bar), and TMAO (open bar) solutions. Osmolyte concentration was 250 mM, and lipid/Aβ ratio was 20:1. Once Aβ was added to the liposome solution in the absence or presence of the osmolytes, the mixture was incubated quiescently for another 1 h at 37 °C.

Figure 6 also shows the effect of osmolytes on permeability. For fresh and 4 h samples, Aβ-induced leakage was reduced to ~10% and ~30% regardless of which osmolyte was used. For the 72 h sample, the osmolytes had no significant effect on membrane leakage. It is interesting to note that the osmolytes had very similar effects on permeability, despite their very different effects on aggregation in the absence of liposomes. This might be because osmolytes alter preformed oligomer distributions or because they modulate the Aβ−membrane interaction.

Osmolyte Effects on Preformed Aggregates. Dissociation of the preformed aggregates was the proposed mechanism for the reduction of Aβ-induced neurotoxicity brought about by trehalose (*17*). To test this hypothesis under our conditions, each of the three osmolytes was added to parallel 4 and 72 h samples to a final concentration of 250 mM. The mixture was then incubated at 37 °C for another hour, and dissolution was assessed by the Congo red binding assay.

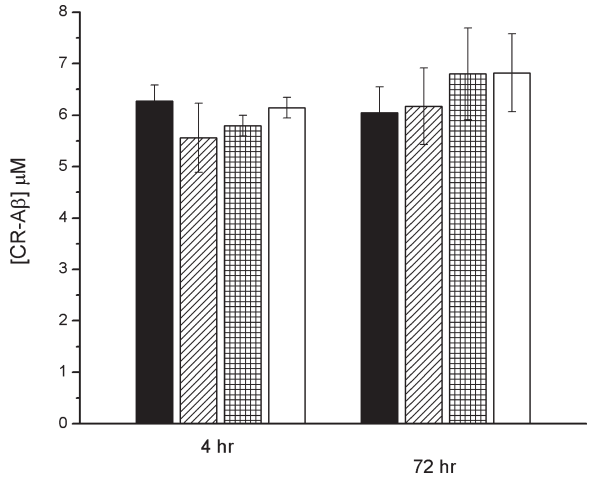

FIGURE 7: Congo red assay of dissolution of preaged Aβ samples by trehalose (slashed bar), sucrose (grid bar), and TMAO (open bar). Aβ samples were incubated for 4 and 72 h in PBS (filled bar). After Aβ sample aggregation, concentrated osmolyte solutions were added to a final concentration of 250 mM, after which osmolytes and aggregated Aβ were allowed to quiescently interact for an additional 1 h at 37 °C. Samples treated with osmolytes are not statistically different from PBS controls (ANOVA, $p > 0.05$).

Congo red binding is unable to distinguish between the presence of oligomers and fibril. However, Congo red does bind to Aβ aggregates instead of monomer, making it useful in differentiating between these two species. Therefore, if aggregates were dissolved back to non-Congo red binding species, the intensity should be significantly reduced. In Figure 7, for both 4 and 72 h samples, Congo red intensities for Aβ controls and samples treated with all three osmolytes were not statistically different. This indicated that an insignificant amount of aggregates was dissolved back to the monomer within the tested time period. To further support the above results, HX-MS was also used to detect the effect of trehalose on 4 and 72 h samples. HX labeling distributions were similar at same labeling time for both samples with or without trehalose, and no increase in the fully labeled peak (monomer) was observed in the trehalose treated samples (see Supporting Information).

HX-MS Analysis. HX-MS was used to determine whether the Aβ oligomer distributions in the presence of lipids could be affected by osmolytes. Aβ in fresh, 4, and 72 h samples were first preaged, then further incubated with POPG or POPC liposomes without CF dye, and finally labeled as described in Materials and Methods for Aβ samples in PBS only. In Figure 8, the mass

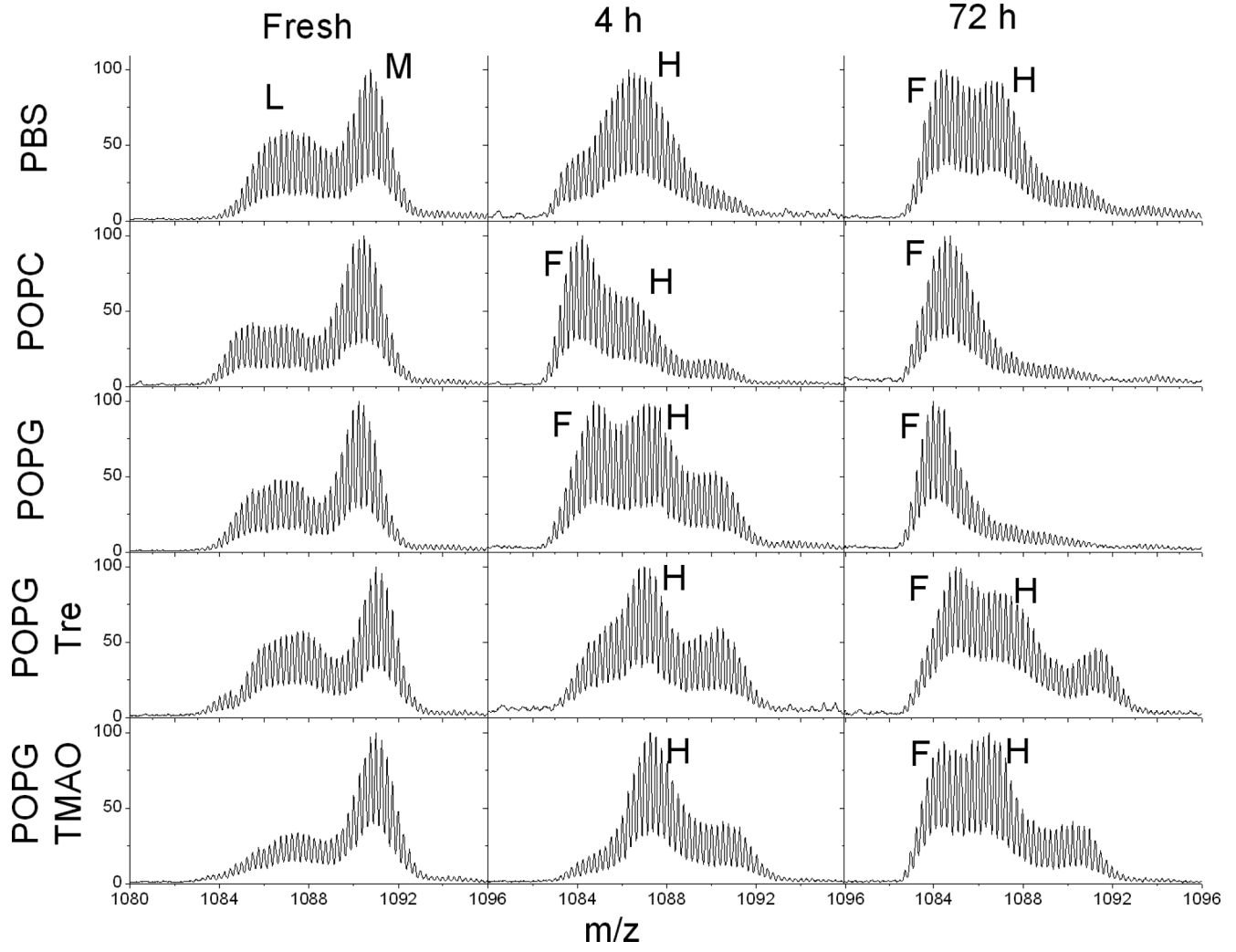

FIGURE 8: Representative hydrogen exchange mass spectra for Aβ samples upon interaction with POPC and POPG LUVs as well as POPG LUVs in the absence and presence of the osmolytes. Labeling time was 10 s for all of the spectra. Preaged Aβ samples in PBS, fresh, 4 and 72 h, are shown in the first row. POPC or POPG liposomes were added to preaged samples with lipid/Aβ molar ratio 10:1 and additional 1 h of incubation at 37 °C. For the fourth and fifth rows, osmolytes and POPG were added to preaged Aβ solution in turn and also incubated for another 1 h 37 °C. Osmolyte concentration was 250 mM for both trehalose and TMAO.

spectra for samples in PBS buffer only (first row, PBS) are shown. In the second and third rows (POPC and POPG), the mass spectra of preaged Aβ samples after incubation with liposomes without osmolytes are displayed. For both kinds of liposomes, fresh Aβ showed a similar HX pattern, indicating either no Aβ−lipid interaction or no effects of the interaction on the initial structural distribution (Figure 8, left column). However, for 4 h incubated Aβ (Figure 8, middle column), a highly protected peak appeared, producing a spectrum similar to that of the 72 h sample in the absence of lipid. For 72 h incubated Aβ, only a fibril peak was observed (Figure 8, right column). Thus, liposomes clearly accelerated Aβ aggregation under our conditions. This was supported by the observation of visible precipitation when Aβ aged for 4 h (see Supporting Information) or 72 h (data not shown) was added to the liposome solution.

Figure 8 also shows how the above acceleration of Aβ aggregation is affected by the presence of osmolytes. Surprisingly, HX labeling distributions in the presence of both osmolytes and liposomes for all incubation times (fresh, 4, and 72 h) (4th and 5th rows) were very similar to those of samples in PBS without liposomes (1st row). Thus, HX-MS shows that both osmolytes abolish the acceleration effect of liposomes on aggregation. This could indicate that they both block the interaction between Aβ and liposomes. Alternatively, since disaccharides in the absence of liposomes appeared to slow down the rate of Aβ aggregation (Figure 2), it is possible that the liposomes and osmolytes have opposing effects on Aβ aggregate distribution and that at least some fraction of the Aβ present interacts with osmolytes and with liposomes. Thus, the results we observed might be a combination of those two effects.

DISCUSSION

Osmolytes are small organic molecules, which in nature stabilize intracellular proteins against environmental stress, such as temperature extremes, dehydration, and high extracellular osmotic pressure (*23*). Recently, certain osmolytes have been shown to increase cell viability in the presence of aggregated Aβ (*17*, *21*) as well as other disease-associated aggregation prone proteins such as α-synuclein and polyglutamine (*20*, *36*). However, the protective effects of osmolytes are still not well understood because of varied conditions between studies as well as limited investigations distinguishing their effects on protein aggregation versus peptide membrane interactions. In this study, we evaluated the effects of selected osmolytes on Aβ-induced membrane permeability, as an *in vitro* surrogate of neurotoxicity. In addition, HX-MS was used to monitor aggregate population distributions in the presence and absence of both liposomes and osmolytes. The overall goal was to determine whether and if possible how each osmolyte affected Aβ−membrane interactions, Aβ aggregation in the absence of liposomes, or both.

The first portion of this work is concerned with examining the effects of osmolytes on Aβ aggregation in the absence of liposomes because Aβ biological activity has been widely assumed to be aggregation state dependent. Two classes of osmolytes, the carbohydrates (sucrose and trehalose) and TMAO had different effects on Aβ aggregation. Disaccharides increased the typical time HMW appeared from 4 h (Figure 2, first row) to 72 h (Figure 2, third and fourth row). However, fibrils were the majority of the sample after 6 days (data not shown) with or without carbohydrates. Hence, disaccharides appear to mainly affect the formation rate of HMW. Furthermore, after 24 h, samples incubated with disaccharides dissociated much more rapidly than controls in PBS (Figure 3). In contrast, TMAO showed little effect on Aβ aggregation. All HX-MS spectra from samples with added TMAO were almost identical to PBS-only controls at the same time points (Figure 2, first and second rows).

The observed reduction in aggregation rate in the presence of disaccharide osmolytes is generally consistent with previous literature reports. Trehalose delayed the aggregation of Aβ(1−40), Aβ(1−42), W7FW14F, and insulin (*17*, *19*). Trehalose and sucrose also attenuated the aggregation of myoglobin containing a 35-glutamine repeat (*20*) and reduced aggregate formation of rhu-mAb HER2 when the sugar/peptide ratio exceeds 500 (*37*). However, under certain conditions, such as low Aβ concentration (10 μM) and different sugar/peptide ratios, sucrose has been found to increase the number of Aβ(1−40) seeds, small aggregates, protofibrils, and fibrils (*22*).

Fewer studies are available on the effects of TMAO on protein aggregation. It has been found to accelerate the Aβ conformation transition from random coil to β-sheet (*38*), α-synuclein aggregation (*39*), and the formation of Tau protein fibrils (*40*). The merely neutral effect of TMAO on Aβ aggregation here is probably attributable to the early appearance of β-sheet structure in our Aβ samples. At the relatively high concentration (100 μM) used here, freshly prepared Aβ contained a significant fraction of protected species termed LMW (Figure 2, first row). Furthermore, CD indicated fresh sample conformation was already β-sheet instead of random coil (refs (*15* and *41*), and Supporting Information). Under similar conditions, the dimer was observed in equilibrium with monomer (*42*). Thus, it is perhaps not surprising that in this case, the TMAO effect on β-sheet formation was not significant.

We then examined the effects of osmolytes on aggregated Aβ induced dye leakage from liposomes and accelerated fibril formation. It should be emphasized that in many studies of Aβ cell and/or liposome interaction, monomeric Aβ was incubated with liposomes or cells, and then viability or/and membrane-induced aggregation was monitored (*8*, *10*, *22*, *25*, *43*). However, in our study, fresh and preaged Aβ samples (4 and 72 h), with well-characterized differences in solvent accessibility and dynamics, were mixed with liposomes in the absence or presence of the tested osmolytes. Since osmolyte effects on Aβ aggregation in the absence of liposomes were specifically studied in an early portion of this article, the above approach allowed us to separate osmolyte effects on aggregation and Aβ aggregate−liposome interactions.

In the absence of osmolytes, we observed that preformed Aβ aggregates induced substantial increases in membrane permeability (Figure 6), with the samples causing the highest CF leakage (fresh and 4 h, Figure 6) having the highest combined fraction of LMW and HMW as measured by HX-MS (Figure 2). This trend is in good agreement with previous reports that Aβ oligomers are particularly effective at increasing vesicle or/and membrane permeability (*2*, *4*, *9*) and causing cell toxicity (*3*, *12*, *14*, *15*, *44*). At the same time, we also found that the liposome interaction clearly accelerated the conversion of HMW to fibrils (Figure 8) as well as visible precipitation under some conditions (see Supporting Information). Such membrane accelerated aggregation was also observed previously in studies carried out without osmolytes (*6*, *10*, *45*).

In the presence of all osmolytes examined, the marked Aβ-induced leakage observed for fresh and 4 h samples was reduced substantially (Figure 6). In addition, the accelerated fibril formation induced by liposomes was abolished by osmolytes

(Figure 8) as was visible precipitation (see Supporting Information). Increased osmotic pressure has been shown previously to reduce leakage from liposomes under different experimental conditions (*46*). While the effect on leakage was much less than that observed in Figure 6, it is possible that osmotic effect is one means by which osmolytes are stabilizing the liposomes.

Effects of trehalose and TMAO on cell toxicity in the presence of the Aβ aggregates have been investigated. At a similar osmolyte/peptide molar ratio, trehalose was found to increase the viability of SY5Y cells (*17*). Likewise, TMAO significantly improved MC56 cell viability under the conditional expression of amyloid precursor protein fragments (*21*). In addition, osmolyte effects of other protein−liposome interactions have been examined. Trehalose decreased the liposome aggregation induced by HSA−liposome interactions (*47*). It reduced lipid vesicle adsorption to polystyrene with only transient intravesicular solute leakage (*48*). It can also block the aggregation of human antibody light chain induced by lipid-derived aldehydes (*49*), which presented in the plasma of AD patients at elevated concentration (*50*) and may also accelerate Aβ aggregation and protofibril formation (*51*). The correlation between our measured trends in dye leakage and the documented benefits to cell viability suggest that membrane permeability effects of osmolytes may play a role in their beneficial effects on cell viability.

HX-MS measurements of the aggregated subpopulation distribution before and after exposure to liposomes were a valuable complement to permeability measurements since they could reveal effects of membrane interactions on the aggregates (*8*, *52*, *53*). The marked reduction in changes in the aggregate distribution upon the addition of osmolytes (Figure 8) suggests that reduction of membrane permeability and/or reduced membrane interactions may be at least one mechanism by which osmolytes reduce Aβ neurotoxicity.

It is important to consider that different aggregated states are thought to differ in their membrane interactions and effects on neurotoxicity (*2*, *4*, *12*, *14*, *15*, *44*, *54*). For example, aggregated Aβ was shown to have greater affinity for the membrane than monomeric Aβ (*52*, *55*). More specifically, only oligomeric intermediates could interact with a lipid bilayer and reduce membrane fluidity (*54*), induce the ion channel activity (*4*), bind to a specific antibody (*14*), and change membrane capacitance (*2*). It was also reported that Aβ-induced liposome aggregation decreased when Aβ was aged for longer times (*56*). Therefore, it was hypothesized that assembly into soluble oligomers generates hydrophobic domains that interact with membranes and that these hydrophobic domains disappear in fibrils (*57*). Our HX-MS and CF leakage data support this hypothesis. LMW oligomers present in fresh samples and HMW oligomers predominant at 4 h were both more solvent exposed (Figure 2) and induced more leakage (Figure 6) than fibrils in the 72 h samples. Proteolytic HX-MS data suggested that the solvent accessibility of residues 1−16 and/or 20−34 is more solvent exposed in the protofibril (*58*) or HMW (*41*) than fibril.

In addition, HX-MS also showed that for both POPC and POPG, HMW was readily converted into a more solvent protected species (Figure 8). It is possible that the solvent inaccessibility due to peptide insertion into lipids could contribute to reduced HX (*59*), but the reduction observed is highly consistent with fibril formation, and the conclusion of accelerated aggregation would be consistent with previous studies (*6*, *10*, *45*). In addition, Aβ aggregates could induce ion channel activity from the liposome made of either neutral or negatively charged lipids (*25*). Thus, accelerated aggregation and ion channel activity with both types of lipids suggest that HMW interacts with either neutral or negatively charged liposomes with similar strength. Measured binding constants for Aβ with POPC and POPG were not statistically different (*52*), and this interaction was regarded to be driven by hydrophobic rather than electrostatic interactions (*53*). CD analysis of preaged Aβ samples upon interaction with POPC liposomes was also carried out (see Supporting Information). No marked conformation change was observed except for a slight intensity increase at 218 nm, consistent with a modest increase in the amount of β-sheet structure when the fibril formed. Thus, during the incubation of preaged Aβ with liposomes, it is possible that little change in secondary structure composition took place other than the assembly of units with β-sheet structure (*41*).

The dissolution of preformed aggregates has been proposed as a competing hypothesis for the beneficial effects of trehalose (*17*). However, under our conditions both Congo red binding (Figure 7) and HX-MS (see Supporting Information) showed that once HMW was formed, it could not be dissolved back to the monomer by adding concentrated osmolytes within 1 h of testing time. In addition, fibril still formed even in the presence of trehalose or sucrose if the incubation time was longer than 6 days (data not shown). Others have also reported that small osmolytes cannot substantially dissolve aggregates. TMAO, PBA (4-phenylbutyric acid), and glycerol were found to protect MC56 cells from Aβ-induced toxicity but did not alter triton insolubility of the aggregate band compared to no treatment (*21*). Thus, under our conditions, the osmolyte's preserving effect on dye leakage cannot be explained by stating that converting preformed Aβ oligomers to monomers. The fact that we did not observe the dissociation of aggregates reported by others (*17*) may be related to the higher Aβ concentration used and faster aggregation observed in our study. Our measurements demonstrated that the osmolytes mainly delayed of the formation of HMW rather than dissolving HMW. Therefore, one possible explanation for the different behavior observed (*17*) is that because of slower aggregation at 20 μM, Aβ samples might still be LMW when trehalose was added after 2 days.

An alternative explanation for the effect of osmolytes on dye leakage from liposomes in the presence of aggregated Aβ is that the osmolytes either increase the stability of oligomers and/or increase the membrane integrity of the liposomes, or both. As discussed earlier, the solvent-exposed hydrophobic patch presented in oligomers may make them less stable kinetically in solution and more likely to interact with lipid membranes. Previous results showed that the intermediate-time incubated samples (4 and 8 h) contain oligomers with lowest apparent stability upon guanidine treatment and also induce the most toxicity in SH-SY5Y cells (*15*). The direct measurement of stability was not carried out in this work. However, the HX-MS data clearly demonstrated that in the presence of the osmolytes, the membrane accelerated transition from HMW to fibril was blocked (Figure 8), and the presence of a more rapidly dissociating LMW species was extended from less than 4 h up to 24 h (Figure 2). Given that without osmolytes samples with the highest content of LMW and HMW induced the most dye leakage (Figure 6), it seems somewhat contradictory that in the presence of osmolytes, the stability of LMW and HMW species are enhanced but dye leakage is attenuated. One explanation for this apparent contradiction is that osmolytes

both enhance the stability of LMW and HMW oligomeric species and reduce their tendency to interact with the lipid membrane surface. This was also proposed to be the possible mechanism of osmolyte action on Aβ by other investigators (*20*, *21*, *60*).

However, those osmolytes may also affect the liposome surface to prevent encapsulated dye leakage, protein adsorption and liposome aggregation (*47*, *48*, *61*). Disaccharides have been shown to associate with the lipid membrane (*62*), form a hydrogen bond to the phosphate groups (*63*), and replace water molecules at the membrane surface (*64*, *65*). TMAO could attenuate membrane disruption, even in the presence of denaturatants such as urea (*66*). Considering the excess amount of osmolyte in the solution as compared to that of Aβ and lipids, it is possible that osmolytes coat on the liposome surface and hence help maintain the membrane integrity (*47*).

Notably, while the different osmolytes had similar effects on dye leakage, TMAO showed different effects on Aβ aggregation in the absence of liposomes. Presumably, the different osmolytes affect the kinetics and/or thermodynamics of steps in the aggregation pathway in a different manner (reviewed by ref *57*). For example, the preferential exclusion of osmolytes has been proposed to be their stabilizing mechanism for globular proteins, but the extent of osmolyte−peptide interaction varies from one osmolyte to another (*23*, *24*, *60*). TMAO is preferentially excluded from both native and denatured states, and forces proteins to fold (reviewed by ref *23*). Sucrose and trehalose have both been shown to shift the conformation equilibrium toward the native state and reduce aggregation (*35*, *60*, *67*). Monomer collapse might be another explanation, but it alone is not necessarily sufficient to protect Aβ from hydrogen exchange (*68*). Thus, it is possible that, in the presence of trehalose and sucrose, the conformational ensemble Aβ was shifted to a set of less aggregation prone conformations and/or that the opportunity for Aβ−Aβ interaction to form large aggregates was reduced.

The detailed mechanism of how each osmolyte exerts their different effects on aggregation kinetics is largely beyond the scope of this article. However, one aspect of the osmolyte−peptide interaction was revealed by adduct formation during electrospray ionization. Aβ/osmolyte adduct formation (Figure 4) was correlated with their delaying effect on aggregation. The differences in osmolyte−peptide interactions are also consistent with the results of a recent transfer free energy model analysis. In this model, TMAO exhibited the highest unfavorable interaction with the peptide backbone, while trehalose and sucrose interact more strongly (*23*, *24*)

While the effects of osmolytes on oligomer distributions and lipid interactions have potential implications for therapeutic strategies, they are not straightforward. In addition, it should be noted that even effective osmolytes such as trehalose may not completely block the formation of neurotoxic oligomers as seen in our results and the work of others (*17*, *19*), nor does it completely attenuate Aβ induced membrane permeability and dye leakage. Therefore, any strategy for modifying the neurotoxic properties and oligomer distribution by such molecules or derivatives will require careful optimization.

ACKNOWLEDGMENT

We thank Dr. Luiz C. Salay, Dr. Alex Lai, and Professor Lukas Tamm for their kind help with the liposome related studies.

SUPPORTING INFORMATION AVAILABLE

HX-MS spectroscopy, CD spectroscopy, and a comparison of Congo red vs HX-MS analysis of aggregates. This material is available free of charge via the Internet at http://pubs.acs.org.

REFERENCES

1. Arispe, N., Diaz, J. C., and Simakova, O. (2007) Aβ ion channels. Prospects for treating Alzheimer's disease with Aβ channel blockers. *Biochim. Biophys. Acta 1768*, 1952–1965.
2. Sokolov, Y., Kozak, J. A., Kayed, R., Chanturiya, A., Glabe, C., and Hall, J. E. (2006) Soluble Amyloid Oligomers Increase Bilayer Conductance by Altering Dielectric Structure. *J. Gen. Physiol. 128*, 637–647.
3. Kayed, R., Sokolov, Y., Edmonds, B., McIntire, T. M., Milton, S. C., Hall, J. E., and Glabe, C. G. (2004) Permeabilization of lipid bilayers is a common conformation-dependent activity of soluble amyloid oligomers in protein misfolding diseases. *J. Biol. Chem. 279*, 46363–46366.
4. Demuro, A., Mina, E., Kayed, R., Milton, S. C., Parker, I., and Glabe, C. G. (2005) Calcium dysregulation and membrane disruption as a ubiquitous neurotoxic mechanism of soluble amyloid oligomers. *J. Biol. Chem. 280*, 17294–17300.
5. Komatsu, H., Liu, L., Murray, I. V. J., and Axelsen, P. H. (2007) A mechanistic link between oxidative stress and membrane mediated amyloidogenesis revealed by infrared spectroscopy. *Biochim. Biophys. Acta 1768*, 1913–1922.
6. Yip, C. M., and McLaurin, J. (2001) Amyloid-β peptide assembly: A critical step in fibrillogenesis and membrane disruption. *Biophys. J. 80*, 1359–1371.
7. Terzi, E., Holzemann, G., and Seelig, J. (1995) Self-association of β-amyloid peptide (1−40) in solution and binding to lipid membranes. *J. Mol. Biol.* 252, 633–642.
8. Terzi, E., Holzemann, G., and Seelig, J. (1997) Interaction of Alzheimer beta-amyloid peptide(1−40) with lipid membranes. *Biochemistry* 36, 14845–14852.
9. McLaurin, J., and Chakrabartty, A. (1996) Membrane disruption by Alzheimer beta: Amyloid peptides mediated through specific binding to either phospholipids or gangliosides. Implications for neurotoxicity. *J. Biol. Chem. 271*, 26482–26489.
10. Bokvist, M., Lindstrom, F., Watts, A., and Grobner, G. (2004) Two types of Alzheimer's β-amyloid (1−40) peptide membrane interactions: Aggregation preventing transmembrane anchoring versus accelerated surface fibril formation. *J. Mol. Biol.* 335, 1039–1049.
11. Ege, C., and Lee, K. Y. C. (2004) Insertion of Alzheimer's A{beta}40 peptide into lipid monolayers. *Biophys. J. 87*, 1732–1740.
12. Bucciantini, M., Giannoni, E., Chiti, F., Baroni, F., Formigli, L., Zurdo, J., Taddei, N., Ramponi, G., Dobson, C. M., and Stefani, M. (2002) Inherent toxicity of aggregates implies a common mechanism for protein misfolding diseases. *Nature 416*, 507–511.
13. Dahlgren, K. N., Manelli, A. M., Stine, W. B., Jr., Baker, L. K., Krafft, G. A., and LaDu, M. J. (2002) Oligomeric and fibrillar species of amyloid-β peptides differentially affect neuronal viability. *J. Biol. Chem. 277*, 32046–32053.
14. Kayed, R., Head, E., Thompson, J. L., McIntire, T. M., Milton, S. C., Cotman, C. W., and Glabe, C. G. (2003) Common structure of soluble amyloid oligomers implies common mechanism of pathogenesis. *Science 300*, 486–489.
15. Lee, S., Fernandez, E. J., and Good, T. A. (2007) Role of aggregation conditions in structure, stability, and toxicity of intermediates in the Abeta fibril formation pathway. *Protein Sci. 16*, 723–732.
16. Kirkitadze, M. D., Bitan, G., and Teplow, D. B. (2002) Paradigm shifts in Alzheimer's disease and other neurodegenerative disorders: The emerging role of oligomeric assemblies. *J. Neurosci. Res. 69*, 567–577.
17. Liu, R., Barkhordarian, H., Emadi, S., Park, C. B., and Sierks, M. R. (2005) Trehalose differentially inhibits aggregation and neurotoxicity of beta-amyloid 40 and 42. *Neurobiology of Disease 20*, 74–81.
18. Arora, A., Ha, C., and Park, C. B. (2004) Inhibition of insulin amyloid formation by small stress molecules. *FEBS Lett. 564*, 121–125.
19. Vilasi, S., Iannuzzi, C., Portaccio, M., Irace, G., and Sirangelo, I. (2008) Effect of trehalose on W7FW14F apomyoglobin and insulin fibrillization: New insight into inhibition activity. *Biochemistry 47*, 1789–1796.
20. Tanaka, M., Machida, Y., Niu, S., Ikeda, T., Jana, N. R., Doi, H., Kurosawa, M., Nekooki, M., and Nukina, N. (2004) Trehalose alleviates polyglutamine-mediated pathology in a mouse model of Huntington disease. *Nature Med. 10*, 148–154.

21. Woltjer, R. L., McMahan, W., Milatovic, D., Kjerulf, J. D., Shie, F.-S., Rung, L. G., Montine, K. S., and Montine, T. J. (2007) Effects of chemical chaperones on oxidative stress and detergent-insoluble species formation following conditional expression of amyloid precursor protein carboxy-terminal fragment. *Neurobiol. Dis. 25*, 427–437.
22. Fung, J., Darabie, A. A., and McLaurin, J. (2005) Contribution of simple saccharides to the stabilization of amyloid structure. *Biochem. Biophys. Res. Commun. 328*, 1067–1072.
23. Bolen, D. W. (2004) Effects of naturally occurring osmolytes on protein stability and solubility: issues important in protein crystallization. *Methods Macromol. Cryst. 34*, 312–322.
24. Street, T. O., Bolen, D. W., and Rose, G. D. (2006) A molecular mechanism for osmolyte-induced protein stability. *Proc. Natl. Acad. Sci. U.S.A. 103*, 13997–14002.
25. de Planque, M. R. R., Raussens, V., Contera, S. A., Rijkers, D. T. S., Liskamp, R. M. J., Ruysschaert, J.-M., Ryan, J. F., Separovic, F., and Watts, A. (2007) β-Sheet structured β-amyloid(1−40) perturbs phosphatidylcholine model membranes. *J. Mol. Biol.* 368, 982–997.
26. Qi, W., Zhang, A., Patel, D., Lee, S., Harrington, J. L., Zhao, L., Schaefer, D., Good, T. A., and Fernandez, E. J. (2008) Simultaneous monitoring of peptide aggregate distributions, structure, and kinetics using amide hydrogen exchange: Application to Abeta(1−40) fibrillogenesis. *Biotechnol. Bioeng.* 100, 1214–1227.
27. Klunk, W. E., Jacob, R. F., and Mason, R. P. (1999) Quantifying amyloid β-peptide (Aβ) aggregation using the Congo Red-Aβ (CR-Aβ) spectrophotometric assay. *Anal. Biochem. 266*, 66–76.
28. Whittemore, N. A., Mishra, R., Kheterpal, I., Williams, A. D., Wetzel, R., and Serpersu, E. H. (2005) Hydrogen-deuterium (H/D) exchange mapping of Aβ amyloid fibril secondary structure using nuclear magnetic resonance spectroscopy. *Biochemistry 44*, 4434–4441.
29. Ambroggio, E. E., Kim, D. H., Separovic, F., Barrow, C. J., Barnham, K. J., Bagatolli, L. A., and Fidelio, G. D. (2005) Surface behavior and lipid interaction of Alzheimer {beta}-amyloid peptide 1−42: A membrane-disrupting peptide. *Biophys. J.* 88, 2706–2713.
30. Weinstein, J. N., Klausner, R., Innerarity, T., Ralston, E., and Blumenthal, R. (1981) Phase transition release, a new approach to the interaction of proteins with lipid vesicles. Application to lipoproteins. *Biochim. Biophys. Acta 647*, 270–284.
31. Walsh, D. M., Hartley, D. M., Kusumoto, Y., Fezoui, Y., Condron, M. M., Lomakin, A., Benedek, G. B., Selkoe, D. J., and Teplow, D. B. (1999) Amyloid beta-protein fibrillogenesis. Structure and biological activity of protofibrillar intermediates. *J. Biol. Chem. 274*, 25945–25952.
32. Lee, S. (2006) Role of Aggregation Conditions and Presence of Small Heat Shock Proteins on Aβ Structure, Stability and Toxicity, in Chemical & Biochemical Engineering , University of Maryland, Baltimore County, Baltimore.
33. Wang, W., Kitova, E. N., and Klassen, J. S. (2005) Nonspecific protein-carbohydrate complexes produced by nanoelectrospray ionization. Factors influencing their formation and stability. *Anal. Chem. 77*, 3060–3071.
34. Zou, Q., Bennion, B. J., Daggett, V., and Murphy, K. P. (2002) The molecular mechanism of stabilization of proteins by TMAO and its ability to counteract the effects of urea. *J. Am. Chem. Soc. 124*, 1192–1202.
35. Lins, R. D., Pereira, C. S., and Hunenberger, P. H. (2004) Trehalose-protein interaction in aqueous solution. *Proteins: Struct., Funct., Bioinf. 55*, 177–186.
36. Sarkar, S., Davies, J. E., Huang, Z., Tunnacliffe, A., and Rubinsztein, D. C. (2007) Trehalose, a novel mTOR-independent autophagy enhancer, accelerates the clearance of mutant huntingtin and {alpha}-synuclein. *J. Biol. Chem. 282*, 5641–5652.
37. Cleland, J. L., Lam, X., J, B. K., Yang, a., Tzung-horng, David, Y., Overcashier, Brooks, D., Hsu, C., and Carpenter, J. F. (2001) A specific molar ratio of stabilizer to protein is required for storage stability of a lyophilized monoclonal antibody. *J. Pharm. Sci. 90*, 310–321.
38. Yang, D.-S., Yip, C. M., Huang, T. H. J., Chakrabartty, A., and Fraser, P. E. (1999) Manipulating the amyloid-beta aggregation pathway with chemical chaperones. *J. Biol. Chem. 274*, 32970–32974.
39. Uversky, V. N., Li, J., and Fink, A. L. (2001) Trimethylamine-N-oxide-induced folding of [alpha]-synuclein. *FEBS Lett. 509*, 31–35.
40. Scaramozzino, F., Peterson, D. W., Farmer, P., Gerig, J. T., Graves, D. J., and Lew, J. (2006) TMAO promotes fibrillization and microtubule assembly activity in the C-terminal repeat region of tau. *Biochemistry 45*, 3684–3691.
41. Zhang, A., Qi, W., Good, T. A., and Fernandez, E. J. (2009) Structural differences between Aβ(1−40) intermediate oligomers and fibrils elucidated by proteolytic fragmentation and hydrogen/deuterium exchange. *Biophys. J.* 96, 1091–1104.
42. Pallitto, M. M., and Murphy, R. M. (2001) A mathematical model of the kinetics of β-amyloid fibril growth from the denatured state. *Biophys. J. 81*, 1805–1822.
43. Kanapathipillai, M., Lentzen, G., Sierks, M., and Park, C. B. (2005) Ectoine and hydroxyectoine inhibit aggregation and neurotoxicity of Alzheimer's β-amyloid. *FEBS Lett. 579*, 4775–4780.
44. Kayed, R., Pensalfini, A., Margol, L., Sokolov, Y., Sarsoza, F., Head, E., Hall, J., and Glabe, C. (2009) Annular protofibrils are a structurally and functionally distinct type of amyloid oligomer. *J. Biol. Chem. 284*, 4230–4237.
45. Koppaka, V., and Axelsen, P. H. (2000) Accelerated accumulation of amyloid β proteins on oxidatively damaged lipid membranes. *Biochemistry 39*, 10011–10016.
46. Niven, R. W., Carvajal, T. M., and Schreier, H. (1992) Nebulization of liposomes 0.3.The effects of operating-conditions and local environment. *Pharm. Res. 9*, 515–520.
47. Bados-Nagy, I., Galantai, R., Laberge, M., and Fidy, J. (2003) Effect of trehalose on the nonbond associative interactions between small unilamellar vesicles and human serum albumin and on the aging process. *Langmuir 19*, 146–153.
48. Adams, D. R., Toner, M., and Langer, R. (2007) Role of trehalose in prevention of giant vesicle adsorption and encapsulated solute leakage in anhydrobiotic preservation. *Langmuir 23*, 13013–13023.
49. Nieva, J., Shafton, A., Altobell, L. J.III, Tripuraneni, S., Rogel, J. K., Wentworth, A. D., Lerner, R. A., and Paul, W. J. (2008) Lipid-derived aldehydes accelerate light chain amyloid and amorphous aggregation. *Biochemistry 47*, 7695–7705.
50. McGrath, L. T., McGleenon, B. M., Brennan, S., McColl, D., McIlroy, S., and Passmore, A. P. (2001) Increased oxidative stress in Alzheimer's disease as assessed with 4-hydroxynonenal but not malondialdehyde. *QJM 94*, 485–490.
51. Chen, K., Kazachkov, M., and Yu, P. H. (2007) Effect of aldehydes derived from oxidative deamination and oxidative stress on β-amyloid aggregation; pathological implications to Alzheimer's disease. *J. Neural. Transm. 114*, 835–839.
52. Kremer, J. J., and Murphy, R. M. (2003) Kinetics of adsorption of β-amyloid peptide Aβ(1−40) to lipid bilayers. *J. Biochem. Biophys. Methods* 57, 159–169.
53. Lin, M.-S., Chiu, H.-M., Fan, F.-J., Tsai, H.-T., Wang, S. S.-S., Chang, Y., and Chen, W.-Y. (2007) Kinetics and enthalpy measurements of interaction between β-amyloid and liposomes by surface plasmon resonance and isothermal titration microcalorimetry. *Colloids Surf., B 58*, 231–236.
54. Kremer, J. J., Pallitto, M. M., Sklansky, D. J., and Murphy, R. M. (2000) Correlation of β-amyloid aggregate size and hydrophobicity with decreased bilayer fluidity of model membranes. *Biochemistry 39*, 10309–10318.
55. Good, T. A., and Murphy, R. M. (1995) Aggregation state-dependent binding of β-amyloid peptide to protein and lipid components of rat cortical homogenates. *Biochem. Biophys. Res. Commun. 207*, 209–215.
56. Kurganov, B., Doh, M., and Arispe, N. (2004) Aggregation of liposomes induced by the toxic peptides Alzheimer's Aβs, human amylin and prion (106−126): facilitation by membrane-bound GM1 ganglioside. *Peptides* 25, 217–232.
57. Murphy, R. M. (2007) Kinetics of amyloid formation and membrane interaction with amyloidogenic proteins. *Biochim. Biophys. Acta 1768*, 1923–1934.
58. Kheterpal, I., Chen, M., Cook, K. D., and Wetzel, R. (2006) Structural differences in Aβ amyloid protofibrils and fibrils mapped by hydrogen exchange-mass spectrometry with on-line proteolytic fragmentation. *J. Mol. Biol. 361*, 785–795.
59. Demmers, J. A. A., Haverkamp, J., Heck, A. J. R., Koeppe, R. E., and Killian, J. A. (2000) Electrospray ionization mass spectrometry as a tool to analyze hydrogen/deuterium exchange kinetics of transmembrane peptides in lipid bilayers. *Proc. Natl. Acad. Sci. U.S.A. 97*, 3189–3194.
60. Kim, Y.-S., Jones, L. S., Dong, A., Kendrick, B. S., Chang, B. S., Manning, M. C., Randolph, T. W., and Carpenter, J. F. (2003) Effects of sucrose on conformational equilibria and fluctuations within the native-state ensemble of proteins. *Protein Sci. 12*, 1252–1261.
61. Wendorf, J. R., Radke, C. J., and Blanch, H. W. (2004) Reduced protein adsorption at solid interfaces by sugar excipients. *Biotechnol. Bioeng. 87*, 565–573.
62. Zhang, P., Klymachyov, A. N., Brown, S., Ellington, J. G., and Grandinetti, P. J. (1998) Solid-state NMR investigations of the glycosidic linkage in α-α' trehalose. *Solid State Nucl. Magn. Reson. 12*, 221–225.

63. Crowe, L. M. (2002) Lessons from nature: the role of sugars in anhydrobiosis. *Comp. Biochem. Physiol., Part A 131*, 505–513.
64. Crowe, L. M., Mouradian, R., Crowe, J. H., Jackson, S. A., and Womersley, C. (1984) Effects of carbohydrates on membrane stability at low water activities. *Biochim. Biophys. Acta 769*, 141–150.
65. Luzardo, M. d. C., Amalfa, F., Nunez, A. M., Diaz, S., Biondi de Lopez, A. C., and Disalvo, E. A. (2000) Effect of trehalose and sucrose on the hydration and dipole potential of lipid bilayers. *Biophys. J. 78*, 2452–2458.
66. Barton, K. N., Buhr, M. M., and Ballantyne, J. S. (1999) Effects of urea and trimethylamine N-oxide on fluidity of liposomes and membranes of an elasmobranch. *Am. J. Physiol. Regul. Integr. Comp. Physiol. 276*, R397–406.
67. Kaushik, J. K., and Bhat, R. (2003) Why is trehalose an exceptional protein stabilizer? An analysis of the thermal stability of proteins in the presence of compatible osmolyte trehalose. *J. Biol. Chem. 278*, 26458–26465.
68. Zhang, S., Iwata, K., Lachenmann, M. J., Peng, J. W., Li, S., Stimson, E. R., Lu, Y. a., Felix, A. M., Maggio, J. E., and Lee, J. P. (2000) The Alzheimer's peptide Aβ adopts a collapsed coil structure in water. *J. Struct. Biol. 130*, 130–141.